Late Paleozoic underplating in North Xinjiang: Evidence from shoshonites and adakites

Zhenhua Zhao *, Xiaolin Xiong, Qiang Wang, Zhenghua Bai, Yulou Qiao

Guangzhou Institute of Geochemistry, Chinese Academy of Sciences, Guangzhou, 510640, China

A B S T R A C T

Shoshonitic series volcanic rocks (SSVR) and adakites are widely distributed in the Permian terrestrial volcanic strata of the Yishijilike–Awulale range of west Tianshan, north Xinjiang, China. Isotopic dating yields Permian ages of 280–250 Ma. The SSVR include absarokite, shoshonite and banakite which are characterized by enrichment of alkalis, particularly in K, combined with lower Ti, higher Al (A/NKC = 0.70–0.99, metaluminous) and $Fe_2O_3 > FeO$. The SSVR that are rich in LILE with high REE contents and Eu/Eu* range from 0.59 to 1.30. They are rich in LREE $((La/Yb)_N$ 2.15–11.97) and depleted in Nb, Ta and Ti (TNT negative anomalies). The adakites are metaluminous to weakly peraluminous (A/NKC = 0.85-1.16) and belong to the high-SiO_2 type of adakite (HSA, $SiO_2 = 62\%$–71%). They are characterized by lower ΣREE with strong LREE enrichment $((La/Yb)_N$ 13–35). Pronounced positive Eu anomalies (Eu/Eu* = 1.02–1.27), very low Yb contents and distinct TNT-negative anomalies are evident. The SSVR have $\varepsilon_{Nd}(t)$ (+1.28 to +4.92) and $(^{87}Sr/^{86}Sr)_i$ (0.7041–0.7057) that are similar to adakites in the regions which are characterized by $\varepsilon_{Nd}(t) = 0.95$ to +5.69 and $(^{87}Sr/^{86}Sr)_i = 0.7050$–0.7053. Trace element, REE and Sr/Nd isotopic compositions suggest that both SSVR and adakites possess similar source regions associated with underplated mantle-derived basaltic materials. Lithosphere extension driven by magmatic underplating was responsible for the generation of both the SSVR and adakites. This magmatism serves as a petrological indicator of underplating during the Permian. Obviously thickened crust (62–52 km), a complex Moho discontinuity, high heat flow (~100 mw·m^{-2}), widespread contemporary alkali-rich granites, basic dike swarms (K–Ar ages of 187–271 Ma, Ar–Ar ages of 174–270 Ma and Rb–Sr ages of 255 ± 28 Ma; $\varepsilon_{Nd}(t)$ +1.84 to +10.1; $(^{87}Sr/^{86}Sr)_i$ 0.7035 and 0.7065), and basic granulites (SHRIMP U–Pb age of 268–279 ± 5.6 Ma) provide additional evidences for the underplating event in this area during Permian.

1. Introduction

Underplating refers to the process of emplacement or addition of mantle-derived basic magma to the base of the lower crust (Furlong and Fountain, 1986; Jin and Gao, 1996). As an important mechanism of crust-mantle interaction and vertical accretion of the crust, the underplating process has attracted a more widespread interest. Granitoids and associated rocks in particular have studied widely in understanding crustal evolution and continental growth (e.g., Stern, 2008; Rino et al., 2008; Ye et al., 2008). Continental growth in the Phanerozoic, particularly the late Paleozoic of the North Xinjiang has attracted much attention since the authors (Zhao et al., 1989, 1993a,b, 2006) first reported that late Paleozoic granitoids along the south margin of the Altay Mountains possess higher $^{143}Nd/^{144}Nd$ and positive $\varepsilon_{Nd}(t)$ and their source region was juvenile crust. The 1998 IGCP-420 Project lead by Prof. Bor-ming Jahn in 1998 promoted an investigation into the

Phanerozoic of North Xinjiang as well as central east Asia orogenic belt (CEAOB), and a suite of late Paleozoic granitoids with high $^{143}Nd/^{144}Nd$ and positive ε_{Nd} (t) were found (Kovalenko et al., 1996; Zhou et al., 1996; Han et al., 1997; Jahn, 1998; Jahn et al., 2000a,b; Chen et al., 2000; Hong et al., 2000; Wu et al., 2000; Chen and Jahn, 2004). Zhao et al. (1993a,b, 1996) proposed that the granites along the south margin of the Altay Mountains resulted from partial melting of juvenile crust and the alkali-rich granites in Ulungur area from higher degree fractional crystallization of depleted-mantle. Han et al. (1997) considered that the alkaline granites were derived from altered depleted-mantle. Zhou et al. (1996) argued that the Alataw granites were derived from the mixing of crust and mantle. In contrast, Hong et al. (2000) suggested new crust formed by subducted ocean crust may have been the source region. The formation mechanism of juvenile crust or mantle-derived materials was widely considered to be related to underplating. Jahn (1998) proposed that the underplating mantle-derived magma interacted and melted together with pre-existing granulite. Han et al., (1996) suggested that the underplating of mantle-derived magma took place on the crust-mantle interface or in the lower crust. Hong et al. (2000) considered that the underplating of basic magma promoted the partial melting of the crust formed by subducted ocean crust prior to 800–600 Ma.

* Corresponding author.
  E-mail address: zhzhao@gig.ac.cn (Z. Zhao).

Additional evidence for the underplating event during the Late Paleozoic in north Xinjiang, has been reported in various studies (Yang et al., 2007; Wang et al., 2008; Xiao et al., 2008; Gao et al., in press). Since 2000, late Paleozoic shoshonitic series volcanic rocks (Zhao et al., 2000, 2004a,b) and adakites (Xiong et al., 2001; Xu et al., 2001; Wang et al., 2003; Zhang et al., 2004; Xiong et al., 2005; Zhang et al., 2005) have been found in North Xinjiang. Zhao et al. (2006) divided the adakites of this area into a subduction-related type and an underplating-related type. The shoshonitic series volcanic rocks (SSVR), underplating-related adakites, alkali-rich granites and alkaline rocks constitute an alkali-rich igneous province in North Xinjiang (Zhao et al., 2000, 2004a,b). Permian (248–292 Ma) bimodal dykes of the adjacent Tarim Basin were recognized which indicate large-scale extension (Li et al., 2008). The late Paleozoic granites in east Tianshan with low $(^{87}Sr/^{86}Sr)_I$ ratios, relative high $^{143}Nd/^{144}Nd$ ratios and association with contemporaneous mafic and ultramafic rocks are related to the underplating event (Wang et al., 2008). From the above, it can be deduced that extensive underplating of mantle-derived magma and obvious continental growth took place during Permian times. These processes are the focus of this paper, which considers the petrology, REE and trace element geochemistry and Sr and Nd isotopic compositions of adakites and (SSVR) together with the data of a global geosciences transect (GGT) across this area, such as thickening crust, complex Moho discontinuity structure and high heat flow.

2. Shoshonitic series volcanic rocks (SSVR) and adakites as an important indicator of continental growth

2.1. Distribution of shoshonitic series volcanic rocks and adakites

The SSVR are mainly distributed in two areas, i.e., Erqisi and West Tianshan volcanic belts. The SSVR in the former are mainly composed of middle Devonian D_2 (Beitashan–D_2b, Yundukara–D_2y and Kasxiweng–D_2k groups), lower Devonian D_1t (Tuoranggekuduke Group) (partly), and lower Carboniferous C_1 (Nanmingshui–C_1n and Batamayineishan–C_1b Groups). Contemporaneous adakites from these areas not discussed in this paper because they are both related to oceanic slab subduction.

The Permian volcanic-sedimentary rocks in Tianshan are mainly composed of basic to acid rocks, which are mostly porphyries, but lack the association of andesite, dacite and rhyolite, and sedimentary rocks containing plant fossils (Zhao Junmen et al., 2003).

The SSVR constitute the majority of Permian volcanic rocks in the region and are mainly distributed in the west Tianshan volcanic belt

where they are concentrated in the Yishijilike–Awulale range (from Kangsugou in the north of Zhaosu county to Naraqin on the east of Nileke county) and the east section of the Nalaqin range (from Nalaqin to Bayinbuluke). The Permian adakites of the Awulale range are mainly distributed in the area from Heishantou to Bugulagou area, around Nileke country. They are less common in the Sanchakou area of East Tianshan. The adakites are temporally and spatially associated with the SSVR, forming an E–W trending belt (Fig. 1).

2.2. Analytical methods

Major element contents were analyzed by conventional wet chemical techniques with precision 2–5%(Li, 1997). The REE and trace elements were determined by a Perkin-Elmer Sciex ELAN 6000 ICP-MS at the Guangzhou Institute of Geochemistry, Chinese Academy of Sciences. About 50 mg of powder sample was dissolved in high-pressure Teflon bomb using a $HF + HNO_3$ mixture. An internal standard solution containing the element Rh was used to monitor the signal drift counting. The USGS standards BCR-1 and BHVO-1 were chosen for calibrating element concentrations. The analytical precision for most elements was generally better than 5% (Liu et al., 1996; Li, 1997).

Sr and Nd isotopic compositions were determined on a Finnigan MAT-262 spectrometer at the Institute of Geology and Geophysics, Chinese Academy of Sciences, using the similar analytical procedure as Li and McColloch (1996). The $^{87}Sr/^{86}Sr$ ratio of standard NBS987 and $^{143}Nd/^{144}Nd$ ratio of the La Jolla standard measured during this study were 0.710234 ± 7 (2σ) and 0.511838 ± 8 (2σ), respectively. Measured $^{87}Sr/^{86}Sr$ and $^{143}Nd/^{144}Nd$ ratios were normalized to $^{87}Sr/^{86}Sr = 0.1194$ and $^{143}Nd/^{144}Nd = 0.7219$, respectively.

The samples for Ar–Ar dating were wrapped in Sn foil and seated in 6-mm-ID evacuated quartz-glass vials together with standard (biotite) flux monitors, and irradiated for 37 h at Beijing Nuclear Research Center. All samples were step-heated using a radio-frequency finance. The Ar isotope analyses were conducted on a MM-1200 mass spectrometer at the Laboratory of Analysis Center, Guilin Resource and Geological Institute. The monitor standard was the ZBH-25 (biotie, 132.5 Ma) and ages were calculated using the constants recommend by Steiger and Jager (1977). All errors are quoted at 1σ level and do not include the uncertainly of the monitor age. The experimental procedures were described by Dai and Hong (1982) and Wang et al. (2003).

The U–Pb isotopic analyses of single zircon were performed using a Perkin-Elmer Sciex ElAN 6000 at Northwest University. A 30–40 μm of

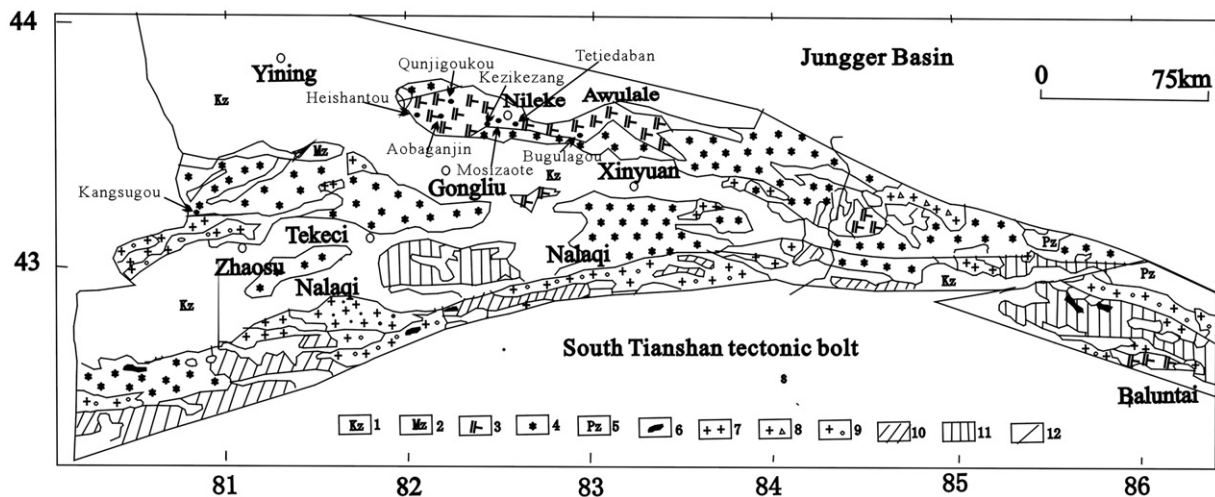Fig. 1. Sketch map showing the distribution of shoshonitic volcanic rocks and adakites in West Tianshan. 1.Cenozoic; 2.Mesozoic; 3. Permian volcanic rocks (adakite, shoshonitic series; 4. Carboniferous volcanic rocks; 5. Proterozoic; 6. Ultramafic rocks; 7. Alkali-rich granites (C_1–P_2); 8. Syenite porphyry; 9. Paleozoic granite; 10. Proterozoic basement; 11. Proterozoic basement; 12. Fault.
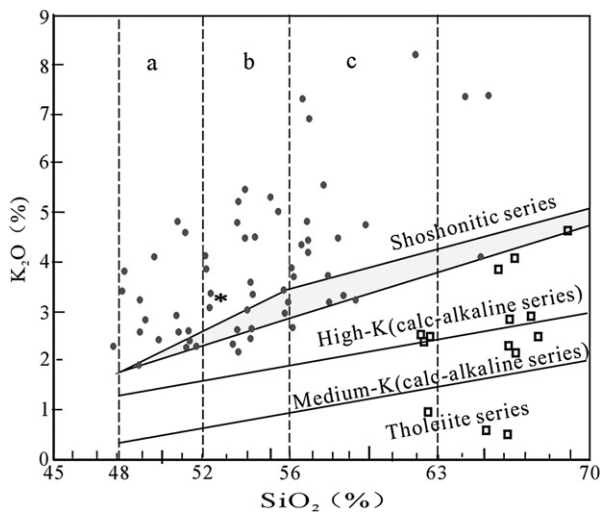
Fig. 2. K_2O–SiO_2 diagram of the shoshonitic series volcanic rocks and adakites in West Tianshan (after Peccerillo and Taylor, 1976; Rickwood, 1989). SSVR Adakites; The shaded area is the field in which fall the boundary lines of Peccerillo and Taylor (1976) and Rickwood (1989): a. Absarokite; b. Shoshonite; c. Banakite.

spot size was adopted. The concentrations of U, Th and Pb were calibrated using ^{29}Si as internal calibrant and NIST SRM 610 as reference material. $^{207}Pb/^{206}Pb$ and $^{206}Pb/^{238}U$ ratios were calculated using GLITTER 4.0 and corrected using the Harvard zircon 91500 as external calibrant (Yuan et al., 2004). U–Pb ages were calculated using ISOPLOT (Ver. 3) (Ludwig, 2003).

2.3. Petrography

2.3.1. Major element chemistry and mineral assemblage of SSVR

The SSVR as discussed here refer to a rock series with SiO_2 48 wt.%– 63 wt.% and K_2O 1.6 wt.%–4.0 wt.% plots in the shoshonite field on the K_2O–SiO_2 diagram (Fig. 2; Peccerillo and Taylor, 1976). They include absarokite, shoshonite and a small amount of banakite, and are characterized by enrichment of alkalis ($K_2O + Na_2O = 5$ wt.%–14 wt.%), particularly K_2O (up to 8.12 wt.%) and $K_2O > Na_2O$ (although $K_2O < Na_2O$ at $SiO_2 < ~50$ wt.%). Most of them have relatively low Ti (mostly < 1.6 wt.%), high Al_2O_3 (ranges from 13 wt.% to 19 wt.%), A/NKC($Al_2O_3/K_2O + Na_2O + CaO$ molecule ratio) = 0.70–0.99 (metaluminous rock) and $Fe_2O_3 > FeO$ (Table 1, Fig. 2). These features are quite similar to those of average shoshonites (Table 1, Morrison, 1980).

The SiO_2 contents of absarokites are 48 wt.%–52 wt.%, which are equivalent to basalts, and $K_2O > 1.6$ wt.%–2.4 wt.%. They are composed of olivine, clinopyroxene, plagioclase, hornblende, magnetite and ilmenite. The clinopyroxene is mainly augite and lesser diopside. Hornblende is mostly altered to chlorite. Microcrystal K-feldspars in the matrix have Ca-sanidine compositions (Ab19.0, An 3.3, Or 77.7). Anorthoclase microcrystals (Ab 64.2, An 7.3, Or 28.5) occur as apomicrocrystals. These rocks show porphyric, micro-ophitic, spor-ophitic and augite glomerophyric textures.

Shoshonite SiO_2 contents are 52 wt.%–56 wt.% and $K_2O > 2.4$ wt.%– 3.2 wt.%, which is equivalent to basaltic andesite. They are composed of olivine, clinopyroxene, plagioclase, magnetite and a small amount of biotite (~1%). The olivine phenocrysts occur as pseudomorphs and were altered to soapstone. Clinopyroxene is augite and plagioclase is typically altered to zoisite. The matrix was mostly devitrified and composed of abundant K-sanidines (Ab 0.8, An 0.5,Or 98.7), plagioclases and anorthoclases (Ab 84.2, An 2.7, Or 13.1). Sporophitic, vitrophyric and hyalopilitic are dominant textures.

SiO_2 contents in banakite are 56 wt.%–63 wt.% (equivalent to andesite in composition) and $K_2O > 3.2$ wt.%–4.0 wt.%. They are composed of olivine (pseudomorph), clinopyroxene, orthopyroxene

and magnetite. The clinopyroxene is augite. Labradorite (An 56.3) plagioclase may exhibt Albite-Carlsband twins. Albitization and zoisitization occur in the matrix of some samples. Microcrystal aggregates of plagioclase occur in the apomatrix with K-feldspar microcrystals (sanidine with Or 99, An1.0, Ab 0). They show porphyritic, poikilitic and vitropilotaxitic textures.

2.3.2. Major element chemistry and mineral assemblage of adakites

The Permian adakites are hypabyssal quartz-albite porphyry, albite porphyry, tonalite, plagioclase granite porphyry and dacite. There are no Nb-enriched basalt (NEB) and high-Mg andesite (HMA) associated with these adakites. These adakites are high-SiO_2 type (HSA, $SiO_2 = 62$ wt.%–71 wt.%, Martin et al., 2005). They possess $Al_2O_3 = 13$ wt.%–16 wt.% with A/NKC = 0.85–1.16, indicating that they are metaluminous to weak peraluminous. Whereas the Sancha-kou adakites in the East Tianshan Mountains are medium-K calc-alkaline series, the Awulaler adakites are notably rich in alkalis, being part of the high-K calc-alkaline series with $K_2O + Na_2O = 6.46$ wt.%– 11.11 wt.% and $Na_2O/K_2O = 1.6$–9.3 (high up to 16) (Fig. 2). MgO contents are lower (< 3.0 wt.%) and Mg# ranges from 35 to 56 (Xiong et al., 2001, 2005). These features are similar to those of underplating-related adakites in Peru and different from those of subduction-related adakites (Mg#55–71; MgO = 1.22–6.78 wt.%; Table 2; Petford and Atherton, 1996).

Plagioclase, hornblende, and less biotite, are the main phenocrysts of the Awulale adakites. The phenocryst plagioclases are typical albite with Ab values of 96.8–98.8. The hornblende phenocrysts are classified as magnesian hornblende with MgO contents greater than 13 wt.%. Magnetite, ilmenite, apatite, zircon and sphene are the main accessory minerals. In the Sanchakou adakites, the plagioclase phenocrysts are andesines with the Ab values of 49.9–55.8 and An values of 43.8–49.6.

2.4. REE and trace element geochemistry

2.4.1. REE geochemistry

Total REE (ΣREE) contents of SSVR are higher and range from 40 ppm to 260 ppm (most of them are 100 ppm) and Eu/Eu* ranges from 0.59 to 1.30 (most of them are ~1.0). They are rich in LREE with $(La/Yb)_N$ ranging from 2.15 to 11.97 (mostly ~5). These features above are closely related to the abundances of major element Si and K. The Eu displays from enrichment to weak-and to moderate depletion. ΣREE and $(La/Yb)_N$ gradually increase with SiO_2 increase but decrease where SiO_2 is higher than 52 wt.%. Chondrite-normalized REE patterns can be divided into four types: HREE enrichment-weak enrichment with Eu moderate depletion ($(La/Yb)_N$ 0.98–4.36; Eu/Eu*0.59–0.74); LREE enrichment with Eu moderate depletion ($(La/Yb)_N$ 3.99–6.00; Eu/Eu*0.79–0.94); both LREE and Eu enrichment ($(La/Yb)_N$ 2.15–5.65; Eu/Eu*1.10–1.30) and LREE obvious enrichment with weak or no Eu depletion($(La/Yb)_N$ 10.77–11.95; Eu/Eu*0.80–1.00)) (Fig. 3, a–d). The third one is mainly for absarokite , the forth for the shoshonite, the first mainly for the banakite and the second for both absarokite and banakite.

The adakites are characterized by lower ΣREE ranging from 50 ppm to 100 ppm (most of them are ~70 ppm) with pronounced LREE enrichment. $(La/Yb)_N$ of Awurale area adakites are 13–35 compared to ~5 for Sanchakou area adakites. Pronounced positive Eu anomalies (Eu/Eu* = 1.02–1.27) and very low Yb contents (0.32 ppm — 1.67 ppm, lower than 1.9 ppm, Defant and Drummond, 1990) are evident in the strongly fractionated chondrite-normalized REE patterns (Table 2, Fig. 3e).

2.4.2. Trace element geochemistry

SSVR are rich in LILE, such as P, Rb, Sr, Ba, Pb, and LREE, which are distinctly higher than those of island arc tholeiite. Th, U, Cr and Ni contents are also higher (Table 1). Compared to the primitive mantle, SSVR are obviously rich in LILE such as K, Rb, Ba and Th and HFSE such

Table 1
Chemical compositions of shoshonitic series volcanic rocks in west Tianshan.

Section	Qunjisayi(2)*	Qunjiguokou(5)	Kezikezang(2)	Aobaganjin(4)	Bugulagou(5)	Kangsugou(4)	Daharaganda(2)	Qiaoerma(3)	Ba'yinbuluke(3)	Average of shosholite (109*)**
SiO_2 (%)	46.45–55.43	49.74–53.25	51.36–53.25	47.75–63.78	45.37–61.25	52.28–55.08	52.68–54.08	52.11–53.13	49.07–53.44	52.41(48–63)
Al_2O_3 (%)	15.72–16.01	13.86–14.56	15.28–16.36	13.77–16.80	15.54–17.07	15.05–16.62	14.78–15.74	17.65–18.62	16.06–17.10	16.17(14–19)
TiO_2 (%)	0.89–1.93	1.40–1.62	1.28–1.62	0.86–1.35	0.40–1.31	0.81–1.45	1.15–1.30	0.81–0.88	0.84–0.86	0.95(<1.3)
K_2O (%)	3.28–4.75	2.34–4.75	2.12–2.60	1.86–7.03	2.18–8.12	2.88–5.34	2.61–2.62	4.71–5.27	2.22–6.53	3.36(1.52–6.05)
Na_2O (%)	2.70–3.53	3.37–5.58	3.52–4.12	2.20–5.28	3.15–6.01	2.17–4.29	3.49–3.51	2.79–3.76	2.80–3.13	3.14(2.05–4.15)
$K_2O + Na_2O$(%)	5.98–8.28	7.31–9.01	5.64–6.72	4.38–10.08	5.33–14.13	6.63–8.70	6.11–6.12	8.06–8.84	5.16–9.66	6.50(>5)
K_2O/Na_2O	1.21–1.35	0.42–1.17	0.60–0.63	0.62–1.63	0.66–1.35	0.77–2.46	0.74–0.75	1.34–1.89	0.76–2.09	1.07(>0.6; >1.0)
Fe_2O_3/FeO	1.49–2.33	3.21–4.17	6.64–9.14	0.85–11.46	0.79–5.24	0.72–1.12	6.42–50.1	1.23–12.22	1.35–43.1	1.03(>0.5)
$Fe_2O_3 + FeO$(%)	9.42–11.72	8.80–11.12	10.25–11.97	5.43–12.44	4.18–15.73	6.98–8.39	8.16–9.70	7.14–8.44	8.38–10.53	7.78
A/NKC	1.07–1.11	0.72–0.98	1.00–1.83	0.88–1.27	0.83–1.49	1.05–1.30	1.00–1.01	1.08–1.20	1.04–1.39	1.04
$\sum$REE(ppm)	120–125	194.5–260.5	80.4–201.2	68–152	56.3–138.9	174.8	183.8	141.9	49.5–134.7	
$(La/Yb)_N$	3.99–4.36	10.8–12.0	4.34–10.81	2.9–4.9	0.98–5.65	7.3	12	6	2.70–3.36	
Eu/Eu*	0.66–0.94	0.80–1.0	0.74–0.89	0.74–0.79	0.59–1.10	0.81	0.84	0.79	0.59–1.18	
Rb (ppm)	96–271	26–100	35–94–	124–289	39–189	108	28	137	112–234	75(24–590)
Ba (ppm)	709–2041	356–2137	723–820	371–960	622–1021	992	686	514	565–608	635(250–1300)
Sr (ppm)	241–890	414–2056	666–748	159–372	60–140	532	601	420	43–513	916(480–2010)
Th (ppm)	1.6–8.8	1.94–4.29	2.43–6.74	2.7–14.3	1.72–20.1	5.24	2.7	11.36	2.58–8.02	2.87(0.79–5.63)
U (ppm)	0.50–2.62	0.86–1.05	0.82–1.9	0.75–3.71	0.47–5.30	1.38	0.68	3.13	0.72–1.76	1.01(0.18–1.93)
Zr (ppm)	192–206	160–195	149–237	82–293	53–550	280	231	169	84–294	91(26–880)
Ni (ppm)	21–75	35–72	20–56	5/16/2008	3–40	21	39	23	4/12/2008	48(4–340)
Co (ppm)	23–38	25–33	26–28	8–35	3/28/2008	20	19	25	6/24/2008	21(8–48)
V (ppm)	206–231	180–227	224–244	64–345	11–234	159	168	149	48–299	244(68–670)
Cr (ppm)	33–76	41–120	48–128	3/23/2008	2–132	25	90	26	12/16/2008	137(2–608)
K/Rb	145–284	308–747	334–508	168–202	354–570	339	777	285	204–255	374(94–1093)
Rb/Sr	0.11–1.12	0.04–0.08	0.05–0.06	0.33–1.8	0.33–3.15	0.2	0.05	0.33	0.22–5.44	0.10(0.02–0.68)
Ba/Rb	2.62–21.3	11.3–27.6	11.3–20.9	2.99–3.32	3.66–15.9	9.19	24.5	3.75	2.60–5.04	9.78(0.48–35)
Th/U	3.22–3.35	1.98–4.56	2.96–4.29	3.57–4.74	2.51–3.79	3.8	3.97	3.63	3.58–4.56	2.66(2.20–3.42)

*Number of sample, **Morrison, 1980.

Table 2
Major, trace elements and REE as well as related parameters of underplating-related adakites in Tianshan, Xinjiang.

Location	Mosizaote	Tetiedaban	Heishantou	Qunjisayi	Sanchakou	Cenozoic or subducted-related adakites (Drummond et al., 1996; Wang et al., 2003)	Underplating-related adakites (Atherton and Petford, 1993)	High-Si adakite (267*) (Martin et al., 2005)
Rock type	Quartz albite porphyry(3*)	Quartz albite porphyry(3)	albite porphyry(4)	Dacite −4	Tonalite porphyry(3)			
SiO_2 (%)	66.88**(65.39–68.74)***	71.00(70.97–71.35)	63.73(62.41–67.04)	66.19(66.39–67.59)	64.54(62.47–66.17)	≥56	56–72	64.8
Al_2O_3(%)	15.88(15.34–16.32)	15.48(15.20–15.70)	15.56(14.17–16.32)	15.51(14.95–15.56)	14.64(13.03–16.27)	17,40, few<15	15–20	16.64
Na/K	1.82(1.41–2.30)	6.82(2.09–14.69)	3.07(1.62–3.75)	2.44(1.90–2.98)	6.76(5.11–8.20)	3.08	1.0–5.6	1.9
A/NKC	0.95(0.87–1.01)	1.10(1.03–1.15)	0.93(0.85–1.15)	1.04(0.92–1.21)	1.14(1.03–1.22)	1.29		1.25
Mg#	47(44–50)	51(48–56)	45(39–48)	52(48–56)	37(35–38)	43		48
MgO%	1.19(1.02–1.37)	1.06(0.93–1.13)	1.82(1.11–2.06)	1.58(1.32–1.75)	1.99(1.83–2.22)	1.22–6.78	0.10–2.56	2.18
Y(ppm)	4.0(4.0–4.0)	5.7(5.0–6.0)	6.5(6.0–7.0)	4.6(3.9–5.)	13.8(12.22–15.17)	≤18	20–15	10
Yb(ppm)	0.33(0.32–0.34)	0.56(0.51–0.59)	0.62(0.54–0.65)	0.37(0.36–0.40)	1.51(1.32–1.67)	≤1.9	0.07–1.03	0.88
Cr(ppm)	6.77(4.36–10.99)	11.0(8.0–13.93)	13.48(9.98–16.41)	12.12(8.45–16.49)	10.85(9.91–12.12)	54		41
Ni(ppm)	14.4(6.19–25.8)	5.6(5.0–6.0)	13.0(6.0–18.49)	9.48(6.84–14.04)	3.21(2.90–3.45)	39		20
Nb(ppm)	1.9(1.8–2.0)	5.3(4.9–5.7)	2.7(2.4–3.5)	2.9(2.5–3.0)	2.09(1.92–2.22)	5.4		6
La/Nb	6.6(4.2–7.9)	2.4(2.0–2.9)	7.9(7.2–8.6)	6.0(5.6–6.5)	5.4(5.2–5.5)	5.5		3.2
$(La/Yb)_N$	29.52(26.91–31.24)	14.91(13.35–16.63)	24.21(21.35–31.45)	30.25(26.31–33.46)	4.9–5.1	≥13	18–96	14.6
Eu/Eu*	1.27(1.26–1.27)	1.06(1.01–1.15)	1.17(1.14–1.21)	1.19(1.16–1.24)	1.10(1.02–1.2)	1.11(0.86–1.34)	≥0.60	0.89
Sr/Y	132(84–194)	59(51–75)	107(66–151)	280(208–327)	57(51–60)	>20–40	38–618	56
V/Sc	8.28(3.68–10.67)	18.3(6.66–36.0)	10.4(7.65–13.0)	10.2(8.17–12.38)	19.2(13.89–22.55)	7.91		

*Number of sample; **average content; ***content range.

as Zr, Hf, but show Nb, Ta and Ti (TNT) negative anomalies relative to the adjacent elements in primitive mantle-normalized spidergram (Fig. 4). The contents of these elements above increase with SiO_2. The SiO_2 content in sample Xt-336 is 61.25 wt.% and the contents of K_2O (8.12 wt.%), Na_2O (6.01 wt.%), Zr (550 ppm), Hf (15.9 ppm), Nb (19 ppm), Ta (1.8 ppm), are the highest contents in all of samples from the area. Y contents are 11–42 ppm and Sr contents are usually lower than 600 ppm, but the Sr contents in shoshonites associated with adakites are higher (600–2056 ppm).

Similar to SSVR, the Permian adakites are significantly enriched in LILE such as K, Rb, Sr, Ba, Th and U in primitive mantle-normalized spidergram. However, the abundances of compatible elements of Cr and Ni (Cr = 4.95–20.4 ppm; Ni = 2.9–25.8 ppm) are distinctly lower than in subducted slab-related adakites of the same area (Cr = 24–132 ppm; Ni = 2.28–45.61 ppm,), or in average Cenozoic average adakites (Cr = 54 ppm, Ni = 39 ppm, Drummond et al., 1996), Their Y contents are also lower (3.9 ppm −15.17 ppm) but Sr contents are higher, resulting in higher Sr/Y (51–336) (Table 2). Both obvious positive Sr anomalies and TNT-negative anomalies occur on primitive mantle-normalized spidergram (Fig. 4).

2.5. Isotopic ages

Isotopic dating was carried out using $^{40}Ar/^{39}Ar$ method for the shoshonites (Table 3). The plateau ages of 5 samples range from 249 Ma to 288 Ma, mostly ~250 Ma (Fig. 5). The isochron ages are between 236 and 277 Ma, indicating they were formed during late Permian (Zhao Junmen et al., 2003).

Rb–Sr, $^{40}Ar/^{39}Ar$ and zircon SHRIMP and LA-ICPMS U–Pb dating gave 248–278 Ma ages of late Permian for adakites (Table 3), which is consistent with those of shoshonites in the same area.

2.6. Sr and Nd isotopic compositions

Sr and Nd isotopic compositions of SSVR and adakites are listed in Table 4. The SSVR and adakites are very similar with higher $(^{143}Nd/^{144}Nd)_i$, positive $\varepsilon_{Nd}(t)$ and lower $(^{87}Sr/^{86}Sr)_i$. For the SSVR, $(^{143}Nd/^{144}Nd)_i$ values range from 0.51232 to 0.51256, $\varepsilon_{Nd}(t)$ from + 1.28 to + 4.92 with lower T_{2DM} (680–883 Ma), $(^{87}Sr/^{86}Sr)_i$ from 0.7041 to 0.7057, $\varepsilon_{Sr}(t)$ from − 0.4 to + 22. There are no obvious differences in the rock units of SSVR. For the adakites, $(^{143}Nd/^{144}Nd)_i$ ranges from 0.51238 to 0.51247, $\varepsilon_{Nd}(t)$ from + 0.86 to + 3.26 with T_{2DM} of 472–699 Ma (the higher $(^{143}Nd/^{144}Nd)_I = 0.51257$ with $\varepsilon_{Nd}(t) = 5.69$ is found in Sanchakou). $(^{87}Sr/^{86}Sr)_i$ change with narrow range of 0.7050–0.7054 but is lower(0.7039) in Sanchakou. These features are quite similar to those of newly underplated basaltic crust-related adakites of Cordillera Blanca Batholith in Peru with $^{143}Nd/^{144}Nd$ range from 0.5125 to 0.5126, $^{87}Sr/^{86}Sr$ from 0.7047 to 0.7057(Petford and Atherton, 1996).

The SSVR and adakites mostly plot in the first quadrant ($\varepsilon_{Nd}(t)>0$, $\varepsilon_{Sr}(t)>0$) near the boundary of the first and second quadrant, and are located to the right of mantle array in diagram of $\varepsilon_{Nd}(t)$ vs. $(^{87}Sr/^{86}Sr)_I$ (Fig. 6). These are different from the potassic igneous rocks (Nelson, 1992) and shoshonitic series rocks in east China (Wang et al., 1996; Zhao and Tu, 2003) but similar to those of Lesser Antilles in Grenada and Vulture and Campania in the Apennines fold belt, Italy (Hawkesworth and Vollmer, 1979) (Fig. 6). The Permian adakites of the Awulale area are different from the subduction-related adakites of North Xinjiang and those of Cenozoic oceanic slab-related adakites world-wide, which mainly plot in the second quadrant along mantle array with higher positive $\varepsilon_{Nd}(t)$ and lower $(^{87}Sr/^{86}Sr))_i<0.7046$ (Fig. 6).

These features imply that the Permian SSVR and adakites in this area possess similar source materials but were not related to oceanic crust subduction. Their source materials were the mantle-derived basic magma underplated onto the crust-mantle interface which
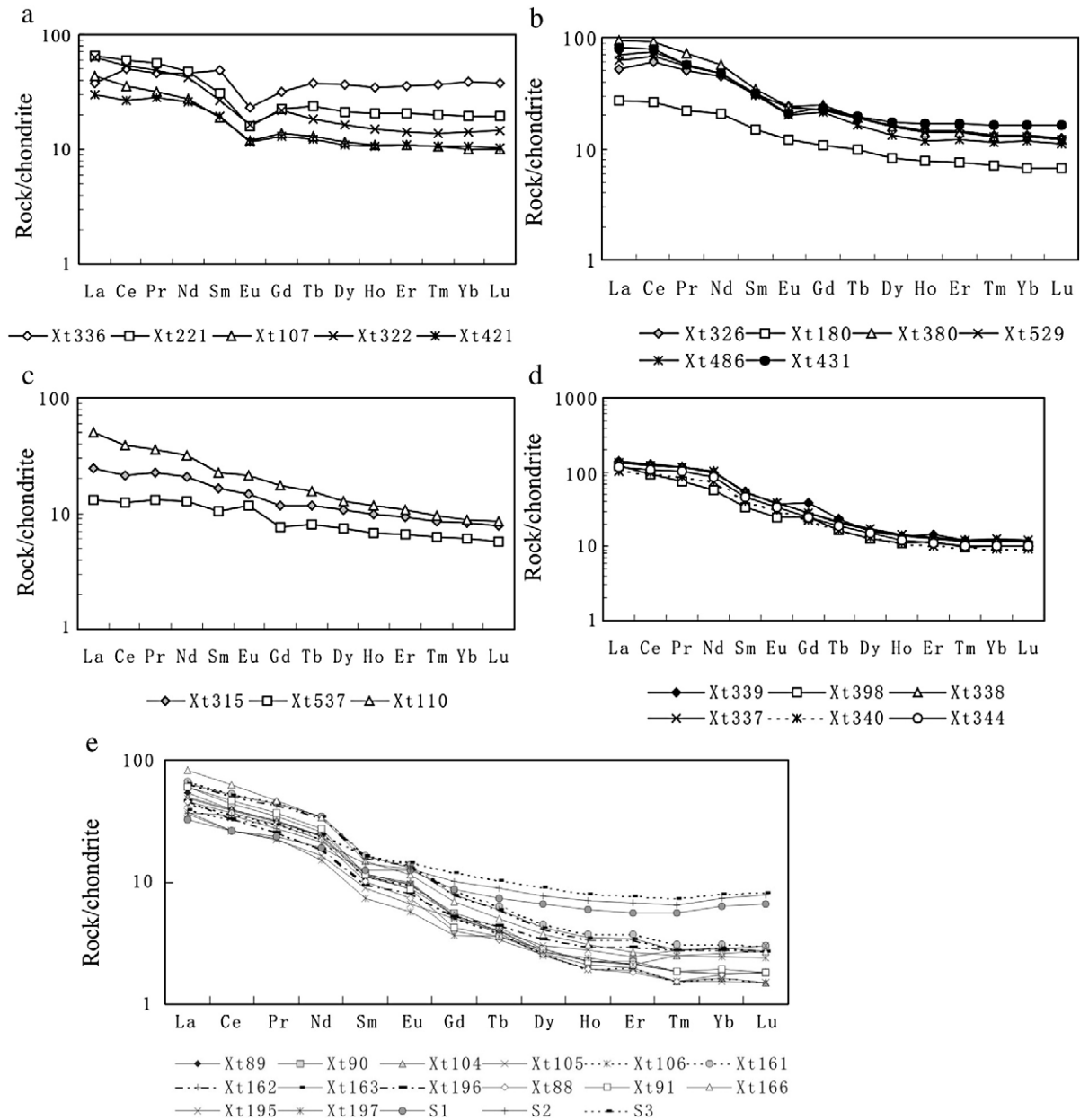
Fig. 3. Chondrite-normalized REE patterns of shoshonitic series volcanic rocks and adakites (normalized -values are from Boyenton, 1984). Shoshonitic series volcanic rocks: a. HREE enrichment-weak enrichment with moderate Eu depletion; b. LREE enrichment with moderate Eu depletion; c. Both LREE and Eu enrichment. d. LREE obvious enrichment with weak or no Eu depletion; Adakites: e. Both LREE and Eu enrichment.

underwent slight contamination by crust materials during their petrogenetic processes.

3. Petrogenetic conditions and tectonic settings of shoshonites and adakites

3.1. Petrogenetic conditions

Experimental data indicates that the distinct K-rich SSVR could not have formed by the partial melting of pyrolite. For instance, they cannot have been produced from low degree partial melting of lherzolite, even under 20–30 kb (70–100 km). For example, 2%–2.5% of partial melting can only yield basanitic magma with SiO_2 contents that do not satisfy the criteria for shoshonite (Wang et al., 1991). Crustal contamination alone also cannot generate K-rich magma from

partial melt originally derived from pyrolite (Wang et al., 1991). The experimental data of Meen (1987, 1990), however, shows that extreme enrichment in K_2O was produced by high degrees of fractional crystallization of basaltic magma under higher pressures. Crystallization of low-Ca pyroxene, olivine, plagioclase and augite can produce K_2O contents of magma that can reach up to 6 wt.% at 10 kb (35 km±) with little increase in SiO_2. Shoshonitic magmas with 3.2 wt.% and 4 wt.%-5 wt.% of K_2O require 85% and 90%–95% high degree fractional crystallization of the basaltic magma with 0.8 wt.% of K_2O, respectively. The contents of SiO_2 and K_2O of SSVR studied in this paper are consistent with the experiment results.

In addition, some trace element ratios, such as higher La/Nb and Pb/Nd (1.3–10.4 and 0.17–5.22, respectively), lower Ce/Pb, Nb/U and Nb/Pb (0.30–9.7, 1.6–16.2 and 0.10–1.47, respectively) (Table 5), are all between those of continental crust and island arc basalt, implying that
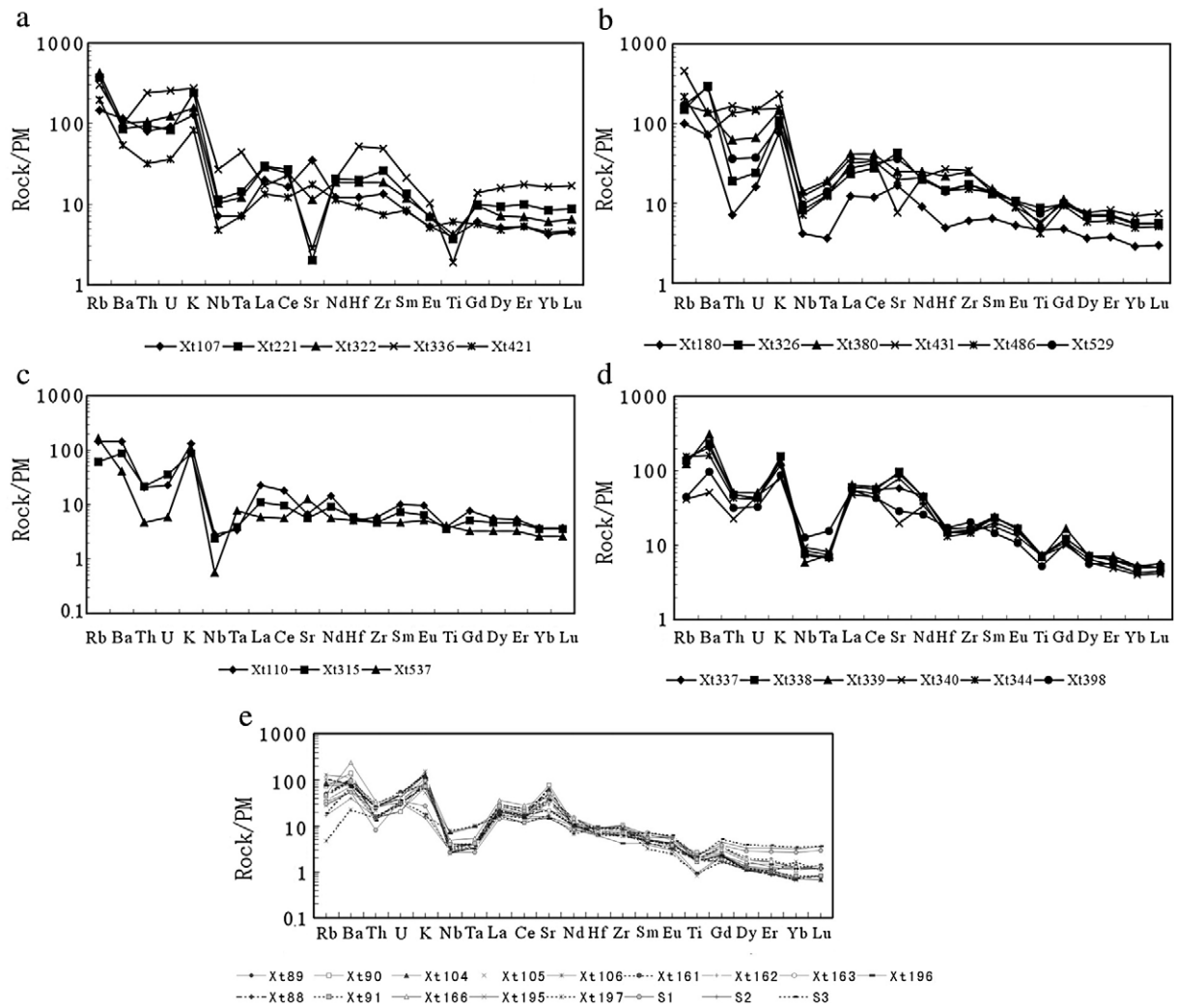
Fig. 4. Primitive mantle-normalized spidergram of trace elements of shoshonitic series volcanic rocks and adakites (normalized-values from Sun and McDonough, 1989).

the magma forming the SSVR had undergone high degrees of fractional crystallization under high pressures (>35 km) and continental crust contamination.

Comparison with the oceanic crust subduction-related adakites, the adakites of this area have higher Na and K, lower MgO (Mg#35–56 with average of 43), more pronounced positive Eu anomalies (Eu/Eu* 1.01–1.27), obvious LREE enrichment ((La/Yb)$_N$ 4.9–32.5) and TNT(Ti, Nd, Ta) negative anomalies. These features indicate that they were generated in the garnet and rutile stablility field and below the plagioclase stability field. It means that they were generated in the transition zone from amphibolite to eclogite, corresponding to 33–50 km and >650 °C (Defant and Dummond, 1990; Rapp et al., 1991; Sen and Dunn, 1994; Rapp and Watson, 1995; Xiong et al., 2001, 2006). The adakitic Cordillera Blanca Batholith derived from the underplating of the late Miocene basaltic materials occurred in the crust that was >50 km thick (Petford and Atherton, 1996).

From the above, the SSVR and adakites have very similar origins and were generated under relatively high pressures (>35 km) from the basaltic magma underplating.

3.2. Source materials

Key diagnostic ratios such as Nb/U, Ce/Pb and Nb/Pb of the SSVR and adakites in the study area are lower and La/Nb and Pb/Nd are higher than those of island arcs and primitive mantle. These ratios are

between those of island arc basalt and lower crust, indicating that continental crust contamination (high Th/Yb and low Ce/Pb ratios) occurred during their petrogenesis process (Table 5).

The trace element ratios are consistent with the Nd and Sr isotopic characteristic of the SSVR and adakites noted above, which are quite

Table 3
Isotopic ages of shoshonites and adakites in Tianshan, Xinjiang.

| Locations	Rocks	Isotopic ages (Ma)		Methods	References
		plateau ages	isochron ages		
Heishantou	Shoshonite	264 ± 5	263 ± 5	$^{40}Ar/^{39}Ar$	This paper
Qunjigoukou	Shoshonite	251 ± 5	236 ± 5	$^{40}Ar/^{39}Ar$	This paper
South Kezikezang	Shoshonite	288 ± 6	277 ± 6	$^{40}Ar/^{39}Ar$	This paper
Kangsugou	Shoshonite	249 ± 4	250 ± 5	$^{40}Ar/^{39}Ar$	This paper
Aobaganjin	Shoshonite	250 ± 4	253 ± 5	$^{40}Ar/^{39}Ar$	This paper
Mosizaote	Adakite	268 ± 5	256 ± 5	$^{40}Ar/^{39}Ar$	This paper
Mosizaote	Adakite	259.5 ± 0.5		zircon LA–ICPMS	This paper
Mosizaote	Adakite		248	Rb–Sr	Li et al. (1998)
Sanchakou	Adakite		278 ± 4	zircon SHRIMP	Li and Chang (1998), Li et al. (2004a,b,c)
Sanchakou	Adakite		276	Rb–Sr	Sun et al. (2002)
Sanchakou	Adakite		269 ± 17	Rb–Sr	Rui et al. (1989, personal communication)
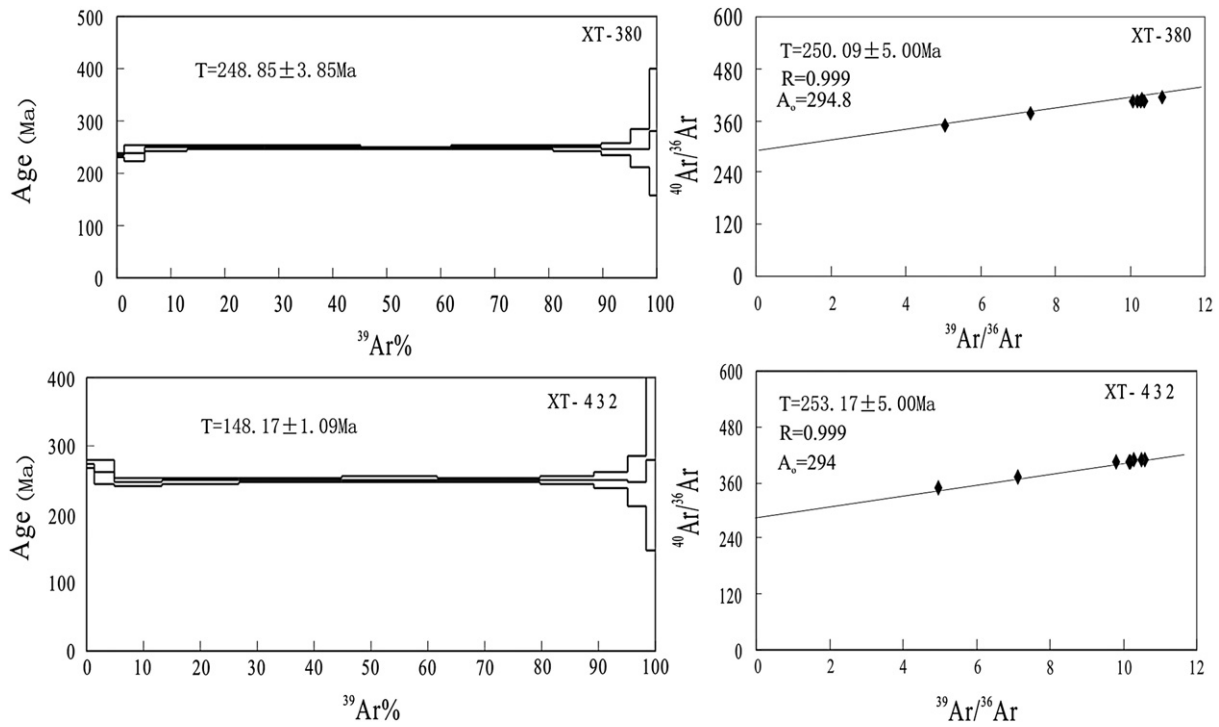
Fig. 5. Plateau and isochron ages of shoshonites.

different from the most potassic volcanic rocks (Nelson, 1992) and the subduction-related adakites in this area, or Aleutian, Cook and Cerro Pamna (Kay, 1978; Kay et al., 1993; Stern and Killian, 1996; Zhao et al., 2006), but are similar to those of underplating-related adakitic Cordillera Blanca Batholith in Peru (Petford and Atherton, 1996).

Collectively, the above trace element and isotopic features imply that the SSVR and adakites in this area had similar source materials, i.e., underplated mantle-derived basalt that underwent continental crust contamination during their petrogenesis.

3.3. Tectonic setting

Both SSVR and adakites occur in the Permian volcanic strata and their isotopic ages confirm late Permian ages for the volcanism (~250 Ma). The Permian volcanic-sedimentary rocks lack the typical

island arc association of andesite, dacite and rhyolite, which may be artributable to the tectonic evolution of Xinjiang Tianshan during the Permian, which involved a transition from a active continental margin to a continental intraplate or post-collisional settings characterized by ocean closure (Han et al., 1996; Zhao et al., 1993a,b; Jahn, 1998; Li and Xiao, 1999; Zhao et al., 2004a,b; Li et al., 2006).

4. Petrologic and geophysical evidences for the underplating in North Xinjiang

4.1. Basic dike swarms and granulite

Basic dyke swarms are an important mark of lithosphere extension (e.g. Hou et al., 2008; Zi et al., 2008). Widespread basic dike swarms occur in granites, particularly in the alkaline granites of the Ulungur,

Table 4
Sr and Nd isotopic compositions of the shoshonitic series volcanic rocks and adakites in North Xinjiang.

| Location	$^{143}Nd/^{144}Nd$	$(^{143}Nd/^{144}Nd)_i$	$\varepsilon_{Nd}(t)$	T_{DM}(Ma)	$(^{87}Sr/^{86}Sr)_i$	References
Adakites						
Mosizaote (3*)	0.512518–0.512547	0.51236–0.51238	−0.82	620–699	0.7054	this paper and Li et al. (1998)
Tetiedaban (2)	0.512589–0.512642	0.51241–0.51247	−1.11	472–571	0.7053	this paper
Heishantou (2)	0.512567–0.512578	0.512405–0.512414	−0.19	568–588	0.7051	this paper
Qunjisayi (3)	0.512556–0.512570	0.51239–0.51241	−0.25	578–598	0.7050–0.7054	this paper
Shanchakou (1)	0.512806	0.51257	5.69	618	0.7039	this paper
Underplating-related adakite		0.5123–0.5126			0.701–0.708	Petford and Atherton (1996)
Subduction-related adakite		>0.5125			<0.7050	Defant et al. (1992), Kay et al. (1993)
Shoshonites						
Qunjisayi	0.512763 ± 6	0.512529	4.4	776	0.7053	this paper
Qunjisayi	0.512911 ± 13	0.512556	4.92	728	0.7057	this paper
Qunjigou	0.512670 ± 10	0.512483	3.51	705	0.7046	this paper
Qunjigou	0.512650 ± 10	0.512461	3.08	742	0.7048	this paper
Kangsugou	0.512580 ± 12	0.51234	1.72	844	0.7054	this paper
Kangsugou	0.512558 ± 14	0.51232	1.28	883	0.7041	this paper
Kangsugou	0.512717 ± 9	0.51247	3.18	680	0.7051	this paper
Kezikezang	0.512642 ± 7	0.51238	2.13	798	0.7054	this paper
Bugulagou	0.512739 ± 15	0.51243	3.38	697	0.7047	this paper

*Number of sample.
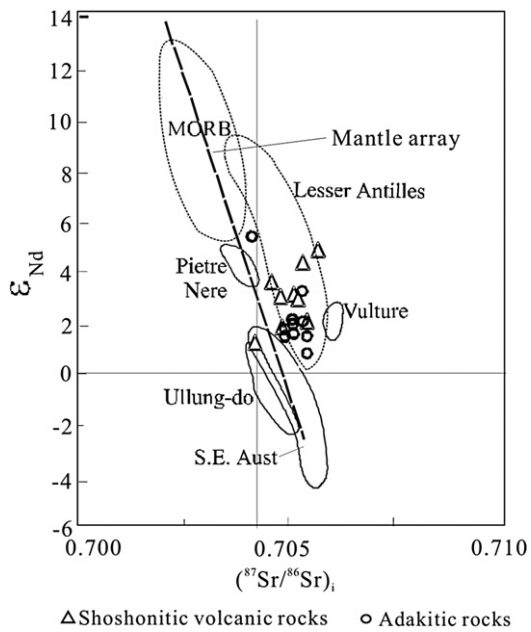
Fig. 6. $\varepsilon_{Nd}(t)$ vs. $(^{87}Sr/^{86}Sr)_i$ diagram of shoshonitic volcanic rocks and adakites in Tianshan, Xinjiang. Lesser Antilles: potassic basalt (Hawkesworth and Vollmer, 1979); Vulture: potassic volcanic rocks, Italy (Hawkesworth et al.1979); S.E.Aust: olivine leucitolith, Australia Nelson (1992); Pietre Nere; alkali volcanic rocks, Italy (Nelson, 1992); ECSP:Mesozoic shoshoinitic series rocks in eastern China (Wang et al., 1996; Zhao et al., 2003; Zhao Junmen et al., 2003); Cenozoic subducted slab related adakite (Defant et al., 1992; Kay et al., 1993; Aguillon-Robles et al., 2001); adakite of Codillera Bianca Betholith (Petford and Atherton, 1996);Carboniferous adakite in Xinjiang Tianshan (Rui et al., 2004; Zhao et al., 2006;Wang et al., 2007).

Sawuershan area on the south margin of Altay Mountain, in the Karamay area of west the Junggar Basin and Tianshan. For example, there are more than 40 mapped basic dykes in the Karamay granites. They are typically several hundreds to thousands of meters in length (longest 6.2 km) and several tens centimeters to several meters wide (0.6–2.5 m) (Qi, 1993; Li et al., 2004a,b,c; Xu et al., 2008; Zhou et al., 2008). These dykes are mainly composed of diabase, diabase porphyry and quartz diorite porphyry with isotopic ages K–Ar of 187–271 Ma (Li et al., 2004a,b,c; Xu et al., 2008), Ar–Ar ages of 174–270 Ma (one sample gave an age of 332 Ma, Zhou et al., 2008) and Rb–Sr 255 ± 28 Ma (Qi, 1993). These ages are consistent with those of SSVR and adakites in this area, i.e., they are mainly later Permian. $\varepsilon_{Nd}(t)$ and $(^{87}Sr/^{86}Sr)_i$ of the these basic dyke swarms range from + 1.84 to + 10.1 and 0.7035–0.7065, respectively (Qi, 1993; Xu et al., 2008). These features indicate that the basic dike swarms resulted from the underplating of mantle-derived magma during the Permian.

Basic granulite is an important constituent of lower crust. It can be produced by strong interaction or metamorphism between lower crust and mantle-derived basaltic magma underplated at the crust-mantle boundary. Accordingly, basic granulite may be an important indicator of an underplating event. In recent years, basic granulites have been found in the southwest Tianshan and Altay area. For instance, basic granulite xenoliths ($SiO_2 = 46$–52 wt.%) were found in Tuoyun, southwest Tianshan, It displays obvious positive Eu anomaly with $Eu/Eu^* = 1.24$ has a U–Pb age (single zircon) of 253 ± 3 Ma (Zheng et al., 2006). Basic granulite found in Wuqiagou, Fuyun County, Altay area, consists of amphibole-plagioclase websterite and pyrox-enite (SiO_2 48–54 wt.%), which has zircon SHRIMP U–Pb age of 268–279 ± 5.6 Ma (Li et al., 2004a,b,c; Chen et al., 2006). These granulite zircon ages are younger than those of metamorphic rocks in the same area, implying that the mafic materials had been added into the lower crust through underplating (Dowens, 1993).

The associations of basic dike swarms and granulites with the Permian alkaline granites, SSVR, adakites and the Permian basalts in

the area and neighbouring areas, such as the Tarim Basin (Li et al., 2008), Tu–Ha Basin and Sangtanghu Basin (Zhou et al., 2006), provided strong petrologic evidence for extensive underplating during the Permian.

4.2. Geophysical evidence on the underplating

Underplating could give rise to variations in geophysically detectable features, such as thickened crust, increased heat flow and complex crust-mantle Moho discontinuity (Dowens et al., 1990; Voshage et al., 1990; Rudnick, 1990a,b). North Xinjiang evolved tectonically in to an intracontinental setting during the late Paleozoic and the present crustal structure of Xinjiang was basically established during the Permian (He et al., 1995). The crust in Tianshan was mainly developed before the Permian (Li and Xiao, 1999). Therefore, the data obtained from the global geoscience transect (GGT) across the west Tianshan could provide an important means of testing the theory that an underplating event took place during late Paleozoic.

4.2.1. Thickening crust

Crustal thickening can result from the underplating, as noted by Dowens et al. (1990) who estimated that the crustal thickness of French Massif Central was increased by 6 km through this process. Underplating is also estimated to have produced 7 km of crustal thickening in the Ivera area, Italy (Voshage et al., 1990, Rudnick, 1990a) and 8 km in Queensland, Australia, corresponding to roughly 17% and 20% of the total crustal thickness in these areas (Rudnick, 1990b). Based on the filtered Bouguer gravity anomalies and seismic data of GGT from Dushanzi (west Tianshan) to Quanshuigou (west Kunlun mountain), the crustal thickness ranges from 62 km to 52 km in the Tianshan area, which is the same of the thickness as the crust in China, and 52 km − 47 km from north Tianshan to the Junggar Basin (Li et al., 2001).

4.2.2. Complex Moho discontinuity structure

Underplating can result in strong interaction at the Moho discontinuity. The superposition or interleaving of underplated basic granulite and basic rocks with anatectic products combined with metamorphism can give rise to a complex Moho discontinuity consisting of a mixed crust-mantle layer or crust-mantle transition zone (Fountain and Salisbury, 1981; Jin and Gao, 1996). Based on the GGT data from Shaya (north margin of Tarim Basin) to Buerjin (south margin of Altay Mountain), the Moho discontinuity is composed of 7–8 thin layers, each of which is 2–3 km in thickness resulting in a complex crust-mantle transitional zone that thickness from south to north to about 20 km beneath west Tianshan. Explosion seismic data obtained at Kuitun (north margin of west Tianshan) also showed that the transitional zone is composed of alternating high and low wave velocity layers (Zhao Junmen et al., 2003). Geoelectromagnetic deep sounding revealed that existence of low velocity and high conductance layers in west Tianshan may be derived from the formation of

Table 5
Trace element ratios of adakites and shoshonites in west Tianshan.

Ratio	Adakite(14)*	Shoshonite(22)	Lower crust**	Island arc basalt (190–359*, Kelemen et al., 2003)	Primitive mantle (Sun and McDonough, 1989)
Ce/Pb	5.34(3.05–14.4) ***	5.00(0.30–9.70)	5	6.96(3.02–21.8)	9.59
Nb/U	3.81(1.84–7.21)	6.00(1.60–16.2)	25	9.88(2.8–22.4)	34
Nb/Pb	0.45(0.19–0.80)	0.57(0.10–1.47)	1.25	1.96(0.44–5)	3.85
Pb/Nb	0.47(0.05–0.75)	0.84(0.19–5.22)	0.36	0.24(0.09–5.0)	0.14
Th/Yb	4.4(2.3–6.7)	1.75(0.40–4.15)	0.8	0.65(0.18–4.20)	0.17
La/Nb	5.9(2.0–8.6)	4.2(1.3–10.4)	1.6	1.62(0.96–2.39)	0.96
Ba/La	39.6(13.8–71.1)	50.5(11.0–125.4)	32.4	24–88(12.9–50.9)	10.2

*Number of sample; **Calculated from Rudnick, 2003.
Mg#>60 for island arc basalt; ***ratio range.

decollement surfaces or partial melting zones, which resulted from the change in the geothermal regime and the rheologic state of the low crust owing to underplating.

4.2.3. High heat flow

Underplating can transfer substantial heat to the lower crust, leading to the formation of a geothermal anomaly. For instance, heat flow in the upper part of the partial melting field resulting from the underplating in the Basin-and-Range area, USA was 2-3 times higher than those of around this area (Jin and Gao, 1996). Extensive occurrences of hot springs and geothermal anomalies in Yellowstone Park, USA, imply this resulted from large scale of basaltic magma underplating (Jin and Gao, 1996). The heat flow is about 100 mw·m^{-2} in the Tianshan orogenic belt distributed SSVR and adakites, which is about twice of the Junggar (41.8–42.3 ± 7.8 mW/m^2 ,Wang et al., 2000; Qiu et al., 2008) and Tarim basins (44.1 mW/m^2 , Wang et al., 1995; Zhao Junmen et al., 2003).

5. Conclusions

The Permian SSVR and adakites with ages 280–250 Ma are widely distributed in the Yishijilike–Awulale area of west Tianshan. Their petrographic associations, trace element, REE and Sr, Nd isotopic compositions preclude generation by subducted-slab melting. Instead, partial melting of newly underplated mantle-derived basaltic materials under high pressures (33–50 km) with or without minor lower crustal contamination in an extensional tectonic setting is a plausible process.

Obvious crustal thickening, complex Moho discontinuity, high crustal heat flow, the occurrence of widespread Permian alkali-rich granites, basic dike swarms and basic granulites provide independent support for the underplating event in this area during the Permian.

Acknowledgements

References

Aquillon-Robles, A., Caimus, T., Bellon, H., Maury, R.C., Cotton, J., Bourgois, J., Michaud, F., 2001. Late Miocene adakite and Nb-enriched basalts from Vizcaino Paninsula, Mexico: indicators of East Pacific Rise subduction below southern Baja California. Geology 29, 531–534.

Atherton, M.P., Petford, N., 1993. Generation of sodium-rich magmas from newly underplated basaltic crust. Nature 362, 144–146.

Boyenton, W.V., 1984. Cosmochemistry of the earth elements: meteorite studies. In: Henderson, R. (Ed.), Rare earth element geochemistry. Developments in geochemistry, vol. 2. Elsevier, Amsterdam, pp. 89–92.

Chen, B., Jahn, B.M., 2004. Genesis of post-collisional granitoids and basement nature of the Junggar Terrane, NW China: Nd-Sr isotope and trace element evidence. Journal of Asian Earth Sciences 23, 691–703.

Chen, J., Zhou, T., Xie, Z., Zhang, X., Guo, X., 2000. Formation of positive eNd (T) granitoids from the Alataw Mountains, Xinjiang, China, by mixing and fractional crystallization: implication for Phanerozoic crustal growth. Tectonophysics 328, 53–67.

Chen, H., Yang, S., Li, Z., Yu, X., Xiao, W., Yuan, C., Lin, X., Li, J., 2006. Zircon SHRIMPU-Pb chronology of Fuyuan basic granulite and its tectonic significance in Altay orogenic belt. Acta Petrologica Sinica 22, 1351–1358.

Dai, T., Hong, A., 1982. ^{40}Ar/^{39}Ar dating and some isotopic determinations on Himalaya biotites from granitoids rocks in south Tibet. Geochimica 11, 48–55 (in Chinese with English abstract).

Defant, M.J., Drummond, M.S., 1990. Derivation of some modern arc magmas by melting of young subducted lithosphere. Nature 347, 662–665.

Defant, M.J., Jackson, T.E., Drummond, M.S., De Boer, J.Z., Bellon, H., Feigenson, M.D., Maury, R.C., Stewart, R.H., 1992. The geochemistry of young volcanism throughout western Panama and southeastern Cost Rica: a review. Journal of the Geological Society (London) 149, 569–579.

Dowens, H., 1993. The nature of lower continental crust of Europe: petrological and geochemical evidence from xenoliths. Physics of the Earth and Planetary Interiors 79, 195–218.

Dowens, H., Deputy, C., Leyreloup, A.F., 1990. Crustal evolution of the Hecynian belt of Western Europe, evidence from lower crustal granulite xenoliths. Chemical Geology 83, 209–231.

Drummond, M.S., Defant, M.J., Kepezhinskas, P., 1996. Petrogenesis of slab-derived trondhjemite-tonalite dacite/adakite magmas. Transactions of the Royal Society of Edingburgh, Earth Science 87, 205–215.

Fountain, D.M., Salisbury, M.H., 1981. Exposed cross-section through the continental crust: implications for crustal structure, petrology and evolution. Earth and Planetary Science Letters 56, 263–267.

Furlong, K.P., Fountain, D.M., 1986. Continental crustal underplating; thermal consideration and seismic- petrologic consequences. Journal of Geophysical Research 91 (B8), 8285–8294.

Gao, J., Long, L., Klemd, R., Qian, Q., Liu, D., Xiong, X., Su, W., Liu, W., Wang, Y., Yan, F., in press. Tectonic evolution of the South Tianshan orogen and adjacent regions, NW China;geochemical and age constraints of granitoid rocks. International Journal of Earth Sciences. DOI 10.1007/s00531.008-0370-8.

Han, B., He, G., Wang, S., 1996. Mantle-derived magmatism, underplating and the nature of basement of Junggar basin. Sci. in China (Series D) 29, 16–21.

Han, B., Wang, S., Jahn, B., Hong, D., Kagami, H., Sun, Y., 1997. Depleted-mantle magma source for the Ulungur River A-type granites from north Xinjiang, China: geochemistry and Nd-Sr isotopic evidence, and implication for Phanerozoic crustal growth. Chemical Geology 138, 135–159.

Hawkesworth, J., Vollmer, R., 1979. Crustal contamination versus enriched mantle: ^{143}Nd/^{144}Nd and ^{87}Sr/^{86}Sr evidence from the Italian volcanics. Earth and Planetary Science Letters 89, 151–165.

He, G., Liu, D., Li, M., Tang, Y., Zhou, R., 1995. The five stage model of crust evolution and metallogenic series of chief orogenic belts in Xinjiang. Xinjiang Geology 13 (2), 99–180 (in Chinese with English abstract).

Hong, D., Wang, S., Xie, X., Zhang, J., 2000. Genesis of positive ε(Nd,t) granitoids in the Da Hinggan Mts-Mongolia Orogenic belt and growth of continental crust. Earth Science Frontiers 7, 441–456 (in Chinese with English abstract).

Hou, G.T., Santosh, M., Quan, X., Lister, G.S., Li, J.H., 2008. Tectonic constraints on 1.3–1.2 Ga final breakup of Columbia supercontinent from a giant radiating dyke swarm. Gondwana Research 14, 561–566.

Jahn, B.M., 1998. Continental growth in the phaneozoic: Nd-Sr isotope evidence from the East-Central Asia orogenic belt, Abstract, 18, IGCP-420 Continental growth in the phanerozoic: Evidence from East-Central ASsia First Workshop.

Jahn, B., Wu, F., Chen, B., 2000a. Massive granitoid generation in Central Asia: Nd isotope evidence and implication for continental growth in the Phanerozoic. Episodes 23, 82–92.

Jahn, B., Griffin, W.L., Windley, B.F., 2000b. Continental growth in the Phanerozoic: evidence from Central Asia special issue. Tectonophysics 328, VII–X.

Jin, Z., Gao, S., 1996. Underplating and it's geodynamical significances for the evolution of crust-mantle boundary. Geological Science and Technology Information 15 (2), 1–7.

Kay, R.W., 1978. Aleutian magnesian andesites: melts from subducted Pacific ocean crust. Journal of Volcanology and Geothermal Research 4, 117–132.

Kay, S.M., Ramos, V.A., Marquez, M., 1993. Evidence in Cerro Pampa volcanic rocks of slab melting prior to ridge trench collision in southern South America. Journal of Geology 101, 703–714.

Kelemen, P.B., Hanghoj, K., Greene, A.R., 2003. In: Holland, H.D., Turekian, K.K. (Eds.), One view of the geochemistry of subduction-related magmatic arcs, with an emphosis on primitive andesite and lower crust. Treatise on geochemistry, vol. 3. Elsevier, Amsterdam, pp. 593–660.

Kovalenko, V.I., Yamolyukv, V., Kovach, V.P., 1996. Sources of Phaneozoic granitoids in central Asia: Sr–Nd isotope data. Geochemistry 8, 699–712 (in Russian).

Li, X., 1997. geochemistry of the Longsheng ophiolite from the southern margin of Yangtze craton, SE China. Geochimical Journal 31, 323–337.

Li, X., McColloch, M.T., 1996. Secular variations in the Nd isotopic composition of Late Proterozoic sediments from the southern margin of the Yangtze Block: evidence for a Proterozoic continental collision in SE China. Precambrian Research 76, 67–76.

Li, J., Xiao, X., 1999. Brief reviews on some issues of framework and tectonic evolution of Xinjiang crust, north China. Scientia Geologica Sinica 34 (4), 405–419 (in Chinese with English abstract).

Li, H., Xie, C., Chang, H., 1998. Study on Metallogenetic Chronology of Nonferrous and Precious Metallic Ore Deposits in North Xinjiang, China. Geological Publishing House, Beijing, pp. 107–127 (in Chinese with English abstract).

Li, Q., Lu, D., Gao, R., Zhang, Z., Liu, W., Li, Y., Li, J., Fan, J., Xiong, X., 2001. An intergrated study of deep seismic sounding profiling along Xinjiang global geoscience transect (Quanshuigou–Dushanzi). Acta Geoscientia Sinica 22, 534–540 (in Chinese with English abstract).

Li, H., Chen, F., Lu, Y., Yang, H., Guo, J., Mei, Y., 2004a. Zircon SHRIMP U–Pb age and strontium isotopes of mineralized granitoids in the Sanchakou copper polymetallic deposit, east Tianshan mountain. Acta Geoscientia Sinica 25 (2), 191–195 (in Chinese with English abstract).

Li, X., Han, B., Ji, J., Li, Z., Liu, Z., Yang, B., 2004b. Geology, geochemistry and K–Ar ages of the Karamay basic-intermediate dyke swarm from Xinjiang, China. Geochimica 33, 574–584 (in Chinese with English abstract).

Li, Z., Chen, H., Yang, S., Xiao, W., Tainosho, Y., 2004c. Discovery of mafic granulites from the Altay orogenic belt: evidence from mineralogical study. Acta Geologica Sinica 20 (6), 1445–1455 (in Chinese with English abstract).

Li, J., He, Gi., Xu, X., Li, H., Sun, G., Yang, T., Gao, L., Zhu, Z., 2006. Crustal tectonic framework of northern Xinjiang and adjacent regions. Acta Geologica Sinica 80 (1), 148–168 (in Chinese with English abstract).

Li, Z., Yang, S., Chen, H., Langmuir, C.H., Yu, X., Lin, X., Li, Y., 2008. Chronology and geochemistry of Taxinan basalts from the Tarim basin: evidence for Permian plume magmatism. Acta Petrologica Sinica 24 (5), 959–970 (in Chinese with English abstract).

Liu, Y., Liu, H., Li, X., 1996. Simultaneous and precise determination of 40 trace elements in rock sample by ICP-MS. Geochimica 25, 552–558.

Ludwig, K.R., 2003. ISOPLOT 3.A geochronological toolkit for Microsoft excel. Berkeley Geochronology Centre Special Publication 4, 74.

Martin, H., Smithies, R.H., Rapp, R., Moyen, J.F., Champion, D., 2005. An overview of adakite, tonalite–trondhjemite–granodiorite(TTG), and sanukitoid: relationships and some implications for crustal evolution. Lithos 79, 1–24.

Meen, J.K., 1987. Formation of shoshonites from calcaline basaltic magma: geochemical and experimental constraints from the type locality. Contributions to Mineralogy and Petrology 97, 333–351.

Meen, J.K., 1990. Elevation of potassium content of basaltic magma by the fractional crystallization: the effect of pressure. Contributions to Mineralogy and Petrology 104, 309–331.

Morrison, G.W., 1980. Characteristics and tectonic setting of the shoshonite rock association. Lithos 13, 97–108.

Nelson, D.R., 1992. Isotopic characteristics of potassic rocks: evidence for the involvement of subducted sediments in magma genesis. Lithos 28, 403–420.

Peccerillo, A., Taylor, S.R., 1976. Geochemistry of Eocene calc-alkaline volcanic rocks from the Kasiamonu area, Northern Turkey. Contributions to Mineralogy and Petrology 58, 68–81.

Petford, N., Atherton, M.P., 1996. Na-rich partial melts from newly underplated basaltic crust: the Cordillera Blanca Batholith, Peru. Journal of Petrology 37, 1491–1521.

Qi, J., 1993. Geology and genesis of vein rock group in western Zhunggar, Xinjiang. Acta Petrologica Sinica 9 (3), 288–298 (in Chinese with English abstract).

Qiu, N., Zhang, Z., Xu, E., 2008. Geothermal regime and Jurassic source rock maturity of the Junggar basin. Journal of Asian Earth Sciences 31, 464–478.

Rapp, R.P., Watson, E.B., 1995. Dehydration melting of metabasalt at 8–32 kbar implications for continental growth and crust–mantle recycling. Journal of Petrology 38, 891–931.

Rapp, R.P., Watson, E.B., Miller, C.F., 1991. Partial melting of amphibolite/eclogite and the origin of Archean trandhjemite and tonalite. Precambrian Research 51, 1–25.

Rickwood, P.C., 1989. Boundary lines within petrologic diagrams which use oxides of major and minor elements. Lithos 22, 247–263.

Rino, S., Kon, Y., Sato, W., Maruyama, S., Santosh, M., Zhao, D., 2008. The Grenvillian and Pan-African orogens: world's largest orogenies through geologic time, and their implications on the origin of superplume. Gondwana Research 14, 51–72.

Rudnick, R.L., 1990a. Nd and Sr isotopic compositions of lower-crustal xenoliths from north Queensland, Australia: implication for Nd model ages and crustal growth processes. Chemical Geology 83, 195–208.

Rudnick, R.L., 1990b. Continental crust: growth from below. Nature 347, 711–712.

Rui, Z., Zhang, L., Chen, Z., Wang, L., Liu, Y., Wang, Y., 2004. Approach on source rock or source region of porphyry copper deposits. Acta Petrologica Sinica 20, 229–238 (in Chinese, with English abstr).

Sen, C., Dunn, T., 1994. Dehydration melting of a basaltic composition amphibolite at 1.5 and 2.0 Gpa: implications for the origin of adakites. Contributions to Mineralogy and Petrology 117, 394–409.

Steiger, R.H., Jager, E., 1997. Subcommission on geochronology convention on the use of decay constants in geo- and cosmochronology. Earth and Planetary Science Letters 36, 359–362.

Stern, R.J., 2008. Neoproterozoic crustal growth: the solid Earth system during a critical episode of Earth history. Gondwana Research 14, 33–50.

Stern, C.R., Killian, R., 1996. Role of the subduction slab, mantle wedge and continental crust in the generation of adakites from the Andean Austral volcanic zone. Contributions to Mineralogy and Petrology 123, 263–281.

Sun, S.S., McDonough, W.F., 1989. Chemical and isotopic systematics of oceanic basalts: implications for mantle composition and processes. In: Saunders, A.D., Norry, M.J. (Eds.), Implications for Mantle Composition and Processes, Magmatism in the Ocean Basins. Geological Society Special Publication, vol. 42, pp. 313–345.

Sun, Y., Tang, X., Mu, J., 2002. Genesis and geochemistry characteristics of copper deposits in Sanchakou, Xinjiang. Mineral Deposits 21 (sup.), 459–462 (in Chinese with English abstract).

Voshage, H., Hoffman, A.W., Mazzucchelli, M., Revalenti, G., Sinigoi, S., Raczek, I., Demarchi, G., 1990. Isotopic evidence from the Ivrea zone for a hybrid lower crust formed by magmatic underplating. Nature 347, 731–736.

Wang, D., Zhou, J., Qiu, J., 1991. The research status of shoshonitic series rocks. Journal of Nanjing Univ (Earth Science) 4, 321–328 (in Chinese with English abstract).

Wang, X., Li, C., Shi, Y., 1995. The characteristics of terrestrial heat flow distribution of Tarim basin. Chinese Journal of Geophysics 38, 855–856 (in Chinese with English abstract).

Wang, D., Ren, Q., Qiu, J., Chen, K., Xu, Z., Zeng, J., 1996. Characteristics of volcanic rocks in the shoshonite province, eastern China, and their metallogenesis. Acta Geologica Sinica 70 (1), 23–34 (in Chinese with English abstract).

Wang, S., Hu, S., Li, T., Wang, J., Zhao, W., 2000. Terrestrial heat flow in Junggar basin, Northwest China. Chinese Science Bulletin 45, 1808–1813.

Wang, Q., Zhao, Z., Bai, Z., Bao, Z., Xu, J., Xiong, X., Mei, H., Wang, Y., 2003. Carboniferous adakites and Nb-enriched arc basaltic rocks association in the Alataw Mountains, north Xinjiang: interactions between slab melt and mantle peridotite and implications for crustal growth. Chinese Science Bulletin 48, 2108–2115.

Wang, Q., Wyman, D.A., Zhao, Z., Xu, J., Bai, Z., Xiong, X., Dai, T., Li, C., Zhu, Y., 2007. Petrogenesis of Carboniferous adakite and Nb-enriched arc basalt in the Alataw area, northern Tianshan Range(west China): implication for Phanerozoic crustal growth in the Central Asia Orogenic belt. Chemical Geology 236, 42–64.

Wang, T., Li, W., Li, J., Hong, D., Tong, Y., Li, S., 2008. Increase of juvenal mantle-derived composition from syn-orogenic to post-orogenic granites of the east part of the eastern Tianshan (China) and implications for the continental vertical growth: Sr and Nd isotopic evidences. Acta Petrologica Sinica 24, 762–772 (in Chinese with English abstract).

Wu, F., Jahn, B., Wilde, S., Sun, D., 2000. Phanerozoic crustal growth: U–Pb and Sr–Nd isotopic evidence from the granites in northeastern China. Tectonophysics 328, 89–113.

Xiao, W., Han, C., Yuan, C., Sun, M., Lin, S., Chen, H., Li, Z., Li, J., Sun, S., 2008. Middle Cambrian to Permian subduction-related accretionary orogenesis of Northern Xinjiang, NW China: Implications for the tectonic evolution of central Asia. Journal of Asian Earth Sciences 32, 102–117.

Xiong, X., Zhao, Z., Bai, Z., Mei, H., Wang, Y., Wang, Q., Xu, J., Bao, Z., 2001. Adakite-type sodium-rich rocks in Awulale Mountain of west Tianshan: Significance for the vertical growth of continental crust. Chinese Science Bulletin 46, 811–817.

Xiong, X., Cai, Z., Niu, H., Chen, Y., Wang, Q., Zhao, Z., Wu, J., 2005. The late Paleozoic adakites in eastern Tianshan area and their metallogenetic significance. Acta Petrologica Sinica 21, 967–976 (in Chinese with English abstract).

Xiong, X., Adam, J., Green, T., Niu, H., Wu, J., Cai, Z., 2006. Trace element characteristics of partial melts produced by melting of metabasalts at high pressures: constrains on the formation condition of adakitic melts. Science in China, Series D 49 (9), 915–925.

Xu, J., Mei, H., Yu, X., Bai, Z., Niu, H., Chen, F., Zhen, Z., Wang, Q., 2001. Adakites related to subduction in the northern margin of Junggar arc for the Late Paleozoic: Products of slab melting. Chinese Science Bulletin 46, 1312–1316.

Xu, Q., Ji, J., Han, B., Zhu, M., Chu, Z., Zhou, J., 2008. Petrology, geochemistry and geochronology of the intermidiate to mafic dykes in north Xinjiang since Late Paleozoic. Acta Petrologica Sinica 24 (5), 977–996 (in Chinese with English abstract).

Yang, S., Li, Z., Chen, H., Santosh, M., Dong, C., Yu, X., 2007. Permian bimodal dyke of Tarim Basin, NW China: Geochemical characteristics and tectonic implications. Gondwana Research 12, 113–120.

Ye, H.-M., Li, X.-H., Li, Z.-X., Zhang, C.-L., 2008. Age and origin of high Ba-Sr appinite-granites at the northwestern margin of the Tibet Plateau: implications for early Paleozoic tectonic evolution of the Western Kunlun orogenic belt. Gondwana Research 13, 126–138.

Yuan, H., Gao, S., Liu, X., Gunthes, D., Wu, F., 2004. Accurate U–Pb age and trace element determinations of zircon by laser-inductively coupled plasma mass spectrometry. Mineralium Deposita 41, 188–200.

Zhang, L., Qin, K., Ying, J., Xia, B., Shu, J., 2004. The relationship between ore-forming processes and adakitic rock in Tuwu-Yandong porphyry copper metallogenic belt, eastern Tianshan Mountains. Acta Petrologica Sinica 20 (2), 259–268 (in Chinese with English abstract).

Zhang, H., Niu, H., Sato, H., Yu, X., Shan, Q., Zhang, B., Ito, J., Nagao, T., 2005. Late Paleozoic adakites and Nb-enriched basalts from northern Xinjiang, northwest China: evidence for the southward subduction of the Paleo-Asian Oceanic Plate. The Island Arc 14, 55–68.

Zhao, J., Liu, G., Lu, Z., Zhang, X., Zhao, G., 2003. Lithospheric structure and dynamic processes of the Tianshan orogenic belt and the Junggar basin. Tectonophysics 376, 199–239.

Zhao, Z., Tu, G., 2003. Supper-large deposits in China. Science Prees, Beijing, pp. 303–371 (in Chinese).

Zhao, Z., Wang, Z., Zou, T.R., 1989. Granitoids and related mineralization in Altay, National-"305" Project report.157-175.

Zhao, Z., Wang, Z., Zou, T., Masuda, A., 1993. The REE, isotopic composition of O, Pb, Sr and Nd and diagenetic model of granitoids in Altay region. In: Tu, G. (Ed.), New improvement of solid geosciences in northern Xinjiang. Science Press, Beijing, pp. 239–266 (in Chinese).

Zhao, Z., Wang, Z., Zou, T., Masuda, A., 1993. study on petrogenesis of alkali-rich intrusive rocks of Ulungur, Xinjiang. Geochimica 25 (3), 205–220 (in Chinese with English abstract).

Zhao, Z., Wang, Z., Zou, T., Masuda, A., 1996. Study on petrogenesis of alkali-rich intrusive rocks of Ulungur, Xinjiang. Geochimica 25, 205–219 (in Chinese with English abstract).

Zhao, Z., Bai, Z., Xiong, X., Mei, H., Wang, Y., 2000. Geochemistry of alkali-rich igneous rocks of northern Xinjiang and its implications for geodynamics. Acta Geologica Sinica 74, 321–328.

Zhao, Z., Bai, Z., Xiong, X., Mei, H., Wang, Y., 2003. $^{40}Ar/^{39}Ar$ chronological study of Late Paleozoic volcanic-hypabyssal igneous rocks in western Tianshan, Xinjiang. Geochimica 32, 317–327 (in Chinese with English abstract).

Zhao, Z., Xiong, X., Wang, Q., Bai, Z., Mei, H., 2004a. A case study on porphyry Cu deposit related with adakite quartz albite porphyry in Moszaote, Western Tianshan, Xinjiang, China. Acta Petrologica Sinica 20, 249–258 (in Chinese with English abstract).

Zhao, Z., Xiong, X., Wang, Q., Bai, Z., Xu, J., Qiao, Y., 2004b. The association of late Paleozoic adakitic rocks and shoshonitic volcanic rocks in Western Tianshan, China. Acta Geologica Sinica 78, 68–72.

Zhao, Z., Wang, Q., Xiong, X., Zhang, H., Niu, H., Xu, J., Bai, Z., Qiao, Y., 2006. Two types of adakites in north Xinjiang, China. Acta Petrologica Sinica 22 (5), 1249–1265.

Zheng, J., Griffin, W.L., O'Reilly, S.Y., Zhang, M., Liou, J.G., Pearson, N., 2006. Granulite xenoliths and their zircons,Tuoyun, NW China: insights into southwestern Tianshan lower crust. Precambrian Research 145, 159–181.

Zhou, T., Chen, J., Li, X., 1996. Origin of high ε_{Nd} granites from Alatao mountain, Xinjiang. Scientia Geologica Sinica 31 (1), 71–79 (in Chinese with English abstract).

Zhou, D., Liu, Y., Xing, X., Hao, J., Dong, Y., Ouyang, Z., 2006. Formation of Permian basalts and implications of geochemical tracing for paleo-tectonic setting and regional tectonic background in the Turpan–Harmi and Santanghu basins, Xinjiang. Science in China (Series D 48 (8), 1146–1157.

Zhou, J., Ji, J., Han, B., Ma, F., Gong, J., Xu, Qi., 2008. $^{40}Ar/^{39}Ar$ geochronology of mafic dykes in north Xinjiang. Acta Petrologica Sinica 24 (5), 997–1010 (in Chinese with English abstract).

Zi, J., Fan, W., Wang, Y., Peng, T., Guo, F., 2008. Geochemistry and petrogenesis of the Permian mafic dykes in the Panxi region, SW China. Gondwana Research 14, 368–382.